Probing oxygen exchange between UiO-66(Zr) MOF and water using 17O solid-state NMR

Florian Venel, Raynald Giovine, Danielle Laurencin, Jessica Špačková, Sébastien Mittelette, Thomas-Xavier Métro, Christophe Volkringer, Olivier Lafon, Frederique Pourpoint

Chemistry–A European Journal
Research Article
doi.org/10.1002/chem.202302731
Chemistry Europe
European Chemical Societies Publishing
www.chemeurj.org

Hot Paper

Probing oxygen exchange between UiO-66(Zr) MOF and water using ^{17}O solid-state NMR

Florian Venel,[a] Raynald Giovine,[a] Danielle Laurencin,[b] Jessica Špačková,[b] Sébastien Mittelette,[b] Thomas-Xavier Métro,[b] Christophe Volkringer,[a] Olivier Lafon,[a] and Frédérique Pourpoint*[a]

The Zr-based Metal Organic Framework (MOF) UiO-66(Zr) is widely employed owing to its good thermal and chemical stabilities. Although the long-range structure of this MOF is preserved in the presence of water during several days, little is known about the formation of defects, which cannot be detected using diffraction techniques. We apply here ^{17}O solid-state NMR spectroscopy at 18.8 T to investigate the reactivity of UiO-66, through the exchange of oxygen atoms between the different sites of the MOF and water. For that purpose, we have selectively enriched in ^{17}O isotope the carboxylate groups of UiO-66(Zr) by using it with ^{17}O-labeled terephthalic acid prepared using mechanochemistry. In the presence of water at 50 °C and a following dehydration at 150 °C, we observe an overall exchange of O atoms between COO^- and μ_3-O^{2-} sites. Furthermore, we demonstrate that the three distinct oxygen sites, μ_3-OH, μ_3-O^{2-} and COO^-, of UiO-66(Zr) MOF can be enriched in ^{17}O isotope by post-synthetic hydrothermal treatment in the presence of ^{17}O-enriched water. These results demonstrate the lability of Zr–O bonds and the reactivity of UiO-66(Zr) with water.

Introduction

More and more researchers are attracted by Metal-Organic Frameworks (MOFs) since they offer many possibilities in terms of structures and pore dimensions. Such tunable materials lead to a large range of physical and chemical properties, due to variable surface areas and chemical stability. Therefore, MOFs represent promising compounds for numerous applications, including catalysis,[1,2] nuclear waste remediation,[3] drug delivery[4,5] and storage and separation of gases.[6] The Zr-based UiO-66 is one of the most widely used MOFs owing to its high thermal and chemical stability compared to other MOFs.[7–12] In particular, its crystalline structure is preserved at conditions of 90% relative humidity and 40 °C over the course of 28 days.[13] This high stability, which is notably crucial for applications in depollution and water treatment, results from the strength of carboxylate-Zr bonds and the high connectivity of the $Zr_6O_4(OH)_4$ clusters, which are capped by twelve terephthalate ligands in the ideal structure (see Figure 1).

As a local characterization technique with an atomic-level resolution, solid-state NMR spectroscopy is a powerful tool to investigate the stability of MOFs in the presence of water, since it allows the observation of defects or amorphous phases, which cannot be detected by diffraction techniques.[14,15] Recently, we notably showed using ^1H NMR that the structure of UiO-66(Zr) MOF is not significantly altered in the presence of water after heating at 50 °C during 48 h, or even at 100 °C during 16 h.[16] We only observed the hydrogen exchange between ZrOH groups and water at 100 °C. Nevertheless, to the best of our knowledge, oxygen exchange between water and UiO-66(Zr) MOF has never been investigated so far, even if the hydrothermal exchange of the ^{17}O isotope between ^{17}O-enriched water and MIL-53(Sc) MOF has been demonstrated and applied for the post-synthetic ^{17}O enrichment of carboxylate and hydroxyl groups.[17]

We investigate herein the exchange of oxygen atoms between water and the UiO-66(Zr) MOF using solid-state NMR of the ^{17}O isotope, which is the only NMR-active isotope of oxygen. The detection of this spin-5/2 quadrupolar nucleus is often prevented by its low natural abundance (0.037%), which strongly limits the sensitivity. Recently, ^{17}O NMR spectra of the MIP-206(Zr) MOF built with isophtalate ligands coordinated to two types of inorganic clusters containing either six or twelve Zr atoms have been recorded in natural abundance, thanks to the sensitivity enhancement provided by dynamic nuclear polarization (DNP) under magic-angle spinning (MAS) conditions.[18] However, these experiments require a specific MAS DNP-NMR spectrometer and the introduction of polarizing agents in the MOF, which can affect its structure and change its hydration state. For instance, it was shown that the μ_3-O sites of MIP-206(Zr) were protonated during the impregnation with an aqueous solution of nitroxide biradicals. Therefore, we rather opted for ^{17}O enrichment of the UiO-66(Zr) MOF. Furthermore,

[a] Dr. F. Venel, Dr. R. Giovine, Prof. Dr. C. Volkringer, Prof. Dr. O. Lafon, Dr. F. Pourpoint
Univ. Lille, CNRS, Centrale Lille, ENSCL, Univ. Artois, UMR 8181 – UCCS – Unité de Catalyse et Chimie du Solide, F-59000 Lille, France
E-mail: frederique.pourpoint@centralelille.fr
[b] Dr. D. Laurencin, Dr. J. Špačková, S. Mittelette, Dr. T.-X. Métro
Institut Charles Gerhardt Montpellier, UMR-5253 CNRS-UM-ENSCM, 1919 route de Mende, 34095 Montpellier, Cedex 05, France

Supporting information for this article is available on the WWW under https://doi.org/10.1002/chem.202302731

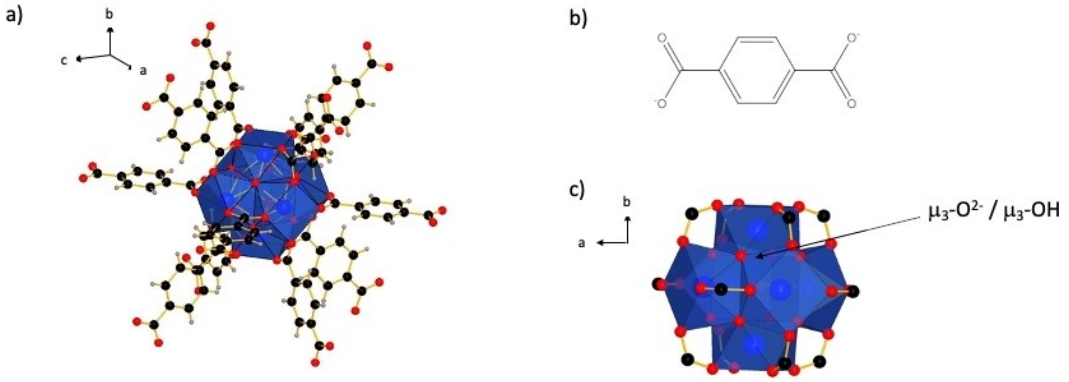

Figure 1. Representation of the atomic-level structure of (a) the 12 terephthalate ligands connected to the inorganic cluster of UiO-66, (b) the terephthalate ligand, and (c) the $Zr_6O_4(OH)_4$ cluster in the ideal structure of UiO-66 MOF. The atoms are displayed with the following colors: zirconium in blue, oxygen in red, carbon in black and hydrogen in gray.

distinct isotopic enrichment levels between the different oxygen sites of the MOF and the water allow monitoring the exchange of oxygen atoms between these sites during hydration and thermal treatment steps.

Various approaches have been proposed for the ^{17}O enrichment of MOFs,[19] including (i) the preparation of ^{17}O-enriched ligands, for instance, by dissolving terephthalic acid in a mixture of acidified ^{17}O-enriched water and dimethylsulfoxide (DMSO), and refluxing the solution for 24 h,[20] (ii) the use of ^{17}O-enriched water during the synthesis of the MOF,[21,22] (iii) the dry gel conversion approach, which limits the amount of ^{17}O-enriched water to approximately 100–200 μL, instead of a few mL in the case of hydrothermal synthesis,[17,21] and (iv) the post-synthetic enrichment by steaming.[17] To the best of our knowledge, the UiO-66(Zr) MOF has only been enriched in ^{17}O by the use of $H_2{}^{17}O$ in a hydrothermal synthesis, involving ~380 mg of terephthalic acid precursor.[21] This approach allowed the ^{17}O enrichment of the three O sites of the UiO-66(Zr) MOF, *i.e.* the carboxylate groups, the μ_3-O^{2-} and the μ_3-OH sites. Nevertheless, it required using 0.25 mL of 40 % ^{17}O-enriched water, which corresponds to a cost of 250 € per NMR sample. However, recently, it was shown that terephthalic acid can be enriched in ^{17}O isotope using mechanochemistry and ^{17}O-enriched water. This approach requires only a few microliters of ^{17}O-enriched water, with a cost of just a few euros to prepare ten milligrams of terephthalic acid, and an average ^{17}O enrichment level of ~20–40 % per oxygen (depending on the enrichment level of the ^{17}O-labeled water used in the synthesis).[23,24] Even if this approach has been applied recently to prepare ^{17}O-enriched non-porous coordination polymers,[25] to the best of our knowledge, it has not yet been demonstrated for the ^{17}O isotopic enrichment of MOFs.

Here, we report the preparation of UiO-66(Zr) MOF, using as a precursor terephthalic acid enriched in ^{17}O isotope by mechanochemistry. ^{17}O solid-state NMR experiments demonstrate the selective enrichment of the carboxylate groups of this MOF. Furthermore, we show the exchange between oxygen atoms of the carboxylate groups and μ_3-O^{2-} sites of UiO-66(Zr) MOF in the presence of water at high temperature (50 and 150 °C). Using ^{17}O-enriched water, we also describe the post-synthetic hydrothermal exchange of oxygen atoms between water and the three O sites of the UiO-66(Zr) MOF. These results reveal the lability of Zr–O bonds in the presence of water, and demonstrate that despite the stability of its crystalline structure, the local structure of the UiO-66(Zr) MOF changes in the presence of water.

Experimental section

The syntheses and treatment procedures for the different samples are summarized in Figures 2 and 3.

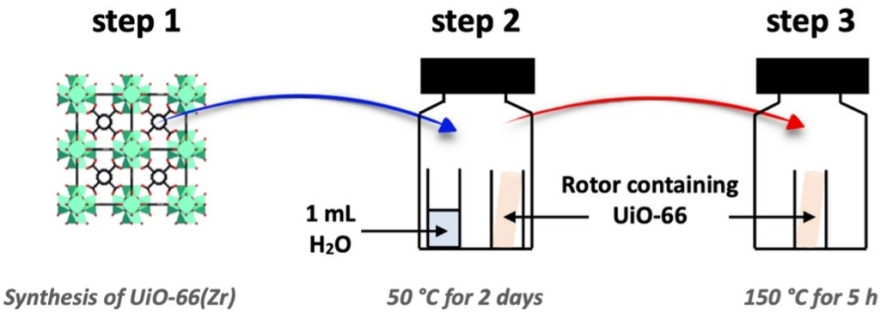

Figure 2. Schematic representation of the three steps corresponding to the synthesis and the hydrothermal treatments of UiO-66(Zr) samples.

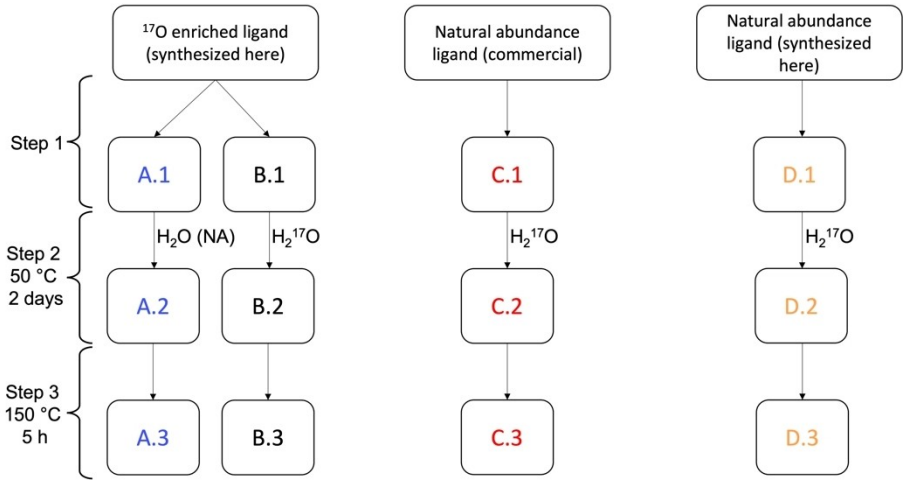

Figure 3. Syntheses and treatment procedures employed for the different investigated samples.

Preparation of ^{17}O-enriched terephthalic acid

Terephthalic acid was enriched in ^{17}O isotope using the recently described mechanochemistry route (1,1-carbonyl-diimidazole (CDI) activation followed by hydrolysis and work-up).[24] This synthesis employed 17 μL of 90% ^{17}O-enriched water to prepare 50 mg of terephthalic acid, which corresponds to a cost of approximately 50 €. The mass spectrometry spectrum of the enriched terephthalic acid is shown in Figure S1. As a control, a non-labeled terephthalic acid precursor was also prepared according to a similar synthetic procedure (CDI activation followed by hydrolysis and work-up), but using non-labeled water as a precursor.

Hydrothermal synthesis and treatments of UiO-66(Zr)

Step 1: synthesis of UiO-66(Zr). The four samples UiO-66(Zr) were synthesized solvothermally, according to the literature procedure.[7] However, the amount of reactant was adjusted to obtain a total volume of 8 mL. Although a modulator (with similar chemical functionalities as the ligand) can be used during the synthesis to control the rate of crystal nucleation and growth,[26] the UiO-66 MOF was synthesized here without any modulator,[7] to limit the number of different O sites in the final material, and also to reduce any possible additional ^{17}O→^{16}O back-exchanges (which would decrease the overall sensitivity of the NMR experiments). For samples A.1 and B.1, we used ^{17}O-enriched terephthalic acid prepared by mechanochemistry, whereas samples C.1 and D.1 were synthesized with non-labeled terephthalic acid, corresponding respectively to a commercial precursor supplied by Fisher Scientific for sample C.1, and to a terephthalic acid precursor which had undergone CDI activation and hydrolysis by mechanochemistry (followed by work-up), just like for the labeling, but using normal (non-enriched) water for sample D.1. For the four samples, 14.1 mg of $ZrCl_4$ (Sigma-Aldrich, 99%) and 19.6 mg of terephthalic acid were dissolved in 1.4 mL of *N*,*N*-dimethylformamide (DMF). The mixture was heated at 120 °C for 24 h, before being centrifugated. The recovered solid was washed three times with anhydrous chloroform. The sample was then transferred in an argon glove box to be packed in a 3.2 mm zirconia rotor for the NMR characterization.

Step 2: adsorption of water. The open rotor was placed in proximity of an open vial of H_2O (1 mL volume) in a closed reactor. Non-labeled water was used for sample A.2, while water enriched in ^{17}O at 70% was used for samples B.2, C.2 and D.2. The 70% ^{17}O-enriched water was purchased from Cortecnet. The system was then heated at 50 °C for 2 days (see Figure 2).

Step 3: heating. The rotors were open and heated at 150 °C for 5 h under air. This final step is identical for all the samples and yields the samples A.3, B.3, C.3 and D.3. After the heating, the rotor was directly closed to perform solid-state NMR.

Solid-state NMR

^{17}O NMR spectra were recorded at 18.8 T, i.e. ^{1}H Larmor frequency of 800 MHz, using a narrow-bore Bruker BioSpin spectrometer equipped with an AVANCE-III console and a 3.2 mm double-resonance HX MAS probe spinning at a MAS frequency, ν_R, of 20 kHz. ^{1}H→^{13}C cross-polarization under MAS (CPMAS) NMR spectra were recorded at 9.4 T (400 MHz for ^{1}H) using a wide-bore Bruker BioSpin spectrometer equipped with an AVANCE-III console and a 3.2 mm double-resonance HX MAS probe spinning at $\nu_R = 20$ kHz. ^{1}H and ^{17}O isotropic chemical shifts were externally referenced respectively to adamantane at 1.7 ppm and H_2O (tap-water) at 0 ppm.

1D ^{17}O NMR spectra were acquired using a single-pulse experiment with a pulse length of 1.85 μs and a radiofrequency (rf) field amplitude of 45 kHz, and resulted from averaging 7,500 or 15,000 transients with a recovery delay of $\tau_{RD} = 1$ s, *i.e.* a total experimental time $T_{exp} = 2$ or 4 h. We also recorded the 1D ^{17}O NMR spectrum of the empty rotor, which exhibits a narrow signal with a chemical shift centered at ~376 ppm (see Figure S2) assigned to OZr_3 sites in tetragonal zirconia.[27]

2D ^{17}O triple-quantum MAS (3QMAS) spectra were acquired using a standard z-filter pulse sequence.[28] The excitation, reconversion and central-transition (CT)-selective pulses of the z-filter lasted 6, 2 and 10 μs with an rf field of 14, 42 and 8 kHz, respectively. The 2D spectra result from averaging 4,608 transients for each of the 40 increments of the indirect evolution period, t_1, with $\tau_{RD} = 1$ s, leading to $T_{exp} = 51.2$ h. The 2D ^{17}O 3QMAS spectra of samples A.1-3 were acquired with a spectral width only allowing the observation of carboxylate signal, whereas those of samples C.3 and D.3 were recorded with a larger spectral width along the direct (F_2) dimension to observe the signals of μ_3-O^{2-}, COO^-, and μ_3-OH sites. Nevertheless, these latter spectra were folded along the indirect (F_1) dimension. Unfolded spectra were plotted by overlapping two spectra processed with shifted spectral window along the F_1

dimension, which explains the lack of noise between 100 and 175 ppm along the F_1 dimension.

2D through-space refocused insensitive nuclei enhancement by polarization transfer (*D*-RINEPT) spectra with ^{17}O excitation and ^{1}H detection ($^{1}H\{^{17}O\}$)[29,30] were acquired using $SR4_1^2$ recoupling,[31] lasting 200 μs, applied on the ^{1}H channel with a nutation frequency of 109 kHz. The π/2 and π pulses on ^{1}H channel, which do not belong to $SR4_1^2$ recoupling, lasted 2.3 and 4.6 μs, respectively, with an rf field amplitude of 36 kHz, while the CT-selective π/2 and π pulses on ^{17}O channel lasted 8.0 and 16.0 μs with an rf field amplitude of 10 kHz. Continuous wave decoupling with a nutation frequency of 109 kHz was applied on ^{1}H channel during the t_1 period. The 2D $^{1}H\{^{17}O\}$ *D*-RINEPT spectra result from averaging 1,056 transients for each 40 t_1-increments and $\tau_{RD} = 1$ s, leading to experimental time $T_{exp} = 11.7$ h.

The 1D $^{1}H \rightarrow ^{13}C$ CPMAS spectra were recorded using an excitation π/2 pulse of 2.5 μs on the ^{1}H channel, and a contact time of 2 ms. During the CP transfer, the nutation frequency on the ^{13}C channel was constant and equal to 100 kHz, whereas the ^{1}H nutation frequency was linearly ramped from 108 to 120 kHz. SPINAL-64 decoupling with a nutation frequency of 78 kHz was applied on the ^{1}H channel during the acquisition of the ^{13}C free-induction decay (FID).[32] The 1D $^{1}H \rightarrow ^{13}C$ CPMAS spectra result from averaging 1024 transients with $\tau_{RD} = 2$ s, i.e. leading to $T_{exp} = 34$ min.

The 1D ^{17}O MAS NMR spectra were simulated using the dmfit software.[33]

FTIR spectroscopy

Fourier-transform infrared (FTIR) analysis was carried out by using a Perkin-Elmer spectrum 2 instrument equipped with a single reflection diamond module (ATR). IR spectra were recorded in the 400–4000 cm^{-1} range with 1 cm^{-1} resolution.

X-ray diffraction

The powder X-ray diffraction XRD patterns were collected at room temperature with a D8 advance A25 Bruker apparatus with a Bragg–Brentano geometry. This diffractometer is equipped with a LynxEye detector with Cu Kα1/α2 radiation. The 2θ range analyzed was 5–50° with a step of 0.02° and a counting time of 0.5 s per step. The calculated powder pattern of UiO-66(Zr) is obtained from the work of Cavka *et al.*[7]

Results and discussion

XRD, IR and $^{1}H \rightarrow ^{13}C$ CPMAS NMR

The XRD powder patterns and IR spectra of the samples A.1, B.1, C.1 and D.1 are displayed in Figure 4a and 4b, respectively. The XRD patterns of all the samples correspond to the one calculated for a UiO-66(Zr) crystalline structure.[7] This result demonstrates that the UiO-66(Zr) MOF can be prepared using a terephthalic acid precursor treated by a protocol involving mechanochemistry steps. The IR spectra of all samples exhibit bands characteristic of the terephthalate ligands and zirconia clusters of the MOF, including the antisymmetric and symmetric stretching of carboxylate groups at 1589 and 1395 cm^{-1}. The slight shift towards low wavenumber for carboxylate stretching modes for samples A.1 and B.1 (compared to C.1 and D.1)

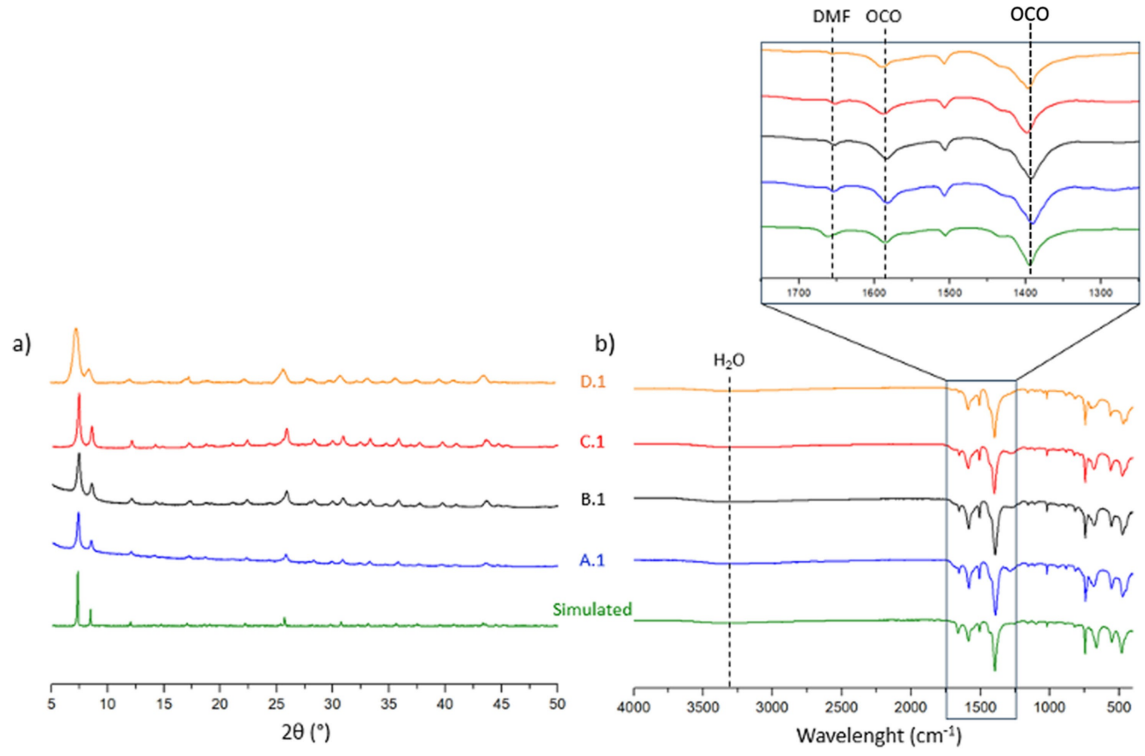

Figure 4. Comparison of experimental (a) XRD powder patterns and (b) FTIR spectra of the four samples after the first step, along with those of the reference structure (green).[7] The dotted lines in FTIR spectra highlight bands attributed to the antisymmetric and symmetric stretching of carboxylate groups at 1589 and 1395 cm^{-1}, the stretching of C=O bond of DMF at 1655 cm^{-1} and to the O–H stretching of the water molecules at ~3300 cm^{-1}.

confirms the higher ^{17}O isotopic enrichment of most carboxylate groups in those samples. We also observe in the experimental IR spectra of Figure 4b a broad band at 3300 cm^{-1} assigned to OH stretching vibrations of water molecules, as well as a band at 1655 cm^{-1} corresponding to the stretching of C=O bond of DMF molecules. These bands evidence the presence of water and DMF in the as-synthesized UiO-66(Zr) MOFs in agreement with previously reported 1D ^{1}H NMR spectra.[16] The 1D $^{1}H\rightarrow^{13}C$ CPMAS NMR spectra of the UiO-66(Zr) samples after the first step are shown in Figure 5a and are dominated by the three ^{13}C signals of the ligand, i.e. those of carboxylate (COO^{-}) and protonated (CH) and non-protonated (C_{α}) aromatic carbon sites. In addition, we observe weak resonances attributed to DMF at 163.6, 35.9 and 30.7 ppm, which confirms the presence of DMF in the pores of UiO-66(Zr) after the synthesis.

The XRD powder patterns and IR spectra of the samples after the second step were not recorded. The XRD powder patterns of the samples after the third step are shown in Figure S3 and show that the crystalline structure of the UiO-66(Zr) is preserved after the (hydro)thermal treatments of the second and third steps. As seen in Figure 5b, the 1D $^{1}H\rightarrow^{13}C$ CPMAS NMR spectra of the samples after the third step are dominated by the three ^{13}C resonances of the terephthalate ligands. The intensity of DMF peaks is reduced since the drying at 150 °C removes a large fraction of DMF molecules adsorbed in the pores. Furthermore, the ligand resonances are broadened with respect to those of the samples after the first step shown in Figure 5a. This broadening suggests a larger distribution of ^{13}C local environments, which may result from the formation of point defects during the hydrothermal treatments or a change in the mobility of the system. Furthermore, a splitting of the ^{13}C resonances of the ligand is observed for the samples A.3 and C.3, which may stem from the presence of free terephthalic acid in these samples in relation with the formation of point defects. The signal intensities of the quaternary $^{13}COO^{-}$ and $^{13}C_{\alpha}$ sites are also reduced after the third step, since the drying at 150 °C removes a large fraction of water and DMF molecules adsorbed in the pores[16] and hence, the density of protons in the vicinity of quaternary carbon atoms is reduced, thus decreasing the efficiency of the CPMAS transfer for these sites.

^{17}O NMR

The 1D ^{17}O MAS spectrum of the sample A.1 is shown in Figure 6. The spectrum of B.1 is identical and hence, is not displayed. This spectrum is dominated by the signal with a maximum peak position at this magnetic field of 275 ppm assigned to the carboxylate group of the terephthalate linkers. Two weak additional signals with a maximum peak position of 389 and 55 ppm are detected and assigned to the μ_3-O^{2-} and μ_3-OH sites, respectively.[21] The μ_3-O^{2-} signal of the MOF masks that of the $^{17}OZr_3$ sites produced by zirconia walls of the MAS rotor (see Figure S2). The much larger intensity of COO^{-} signal compared to those of μ_3-O^{2-} and μ_3-OH sites indicates that the carboxylate oxygen atoms remain selectively labeled in ^{17}O isotope when UiO-66(Zr) MOF is synthesized using our procedure, starting from an ^{17}O-enriched terephthalic acid. Indeed, the weak intensity of the μ_3-OH and μ_3-O^{2-} signals indicates that the oxygen isotopic exchange between COO^{-} groups and those sites is limited during the synthesis. The 2D ^{17}O 3QMAS spectrum of sample A.1 shown in Figure 8a confirms the presence of a main COO^{-} signal with NMR parameters similar to those previously reported for this ^{17}O site.[21]

The ^{1}H-^{17}O proximities in sample A.1 were also probed by recording a 2D ^{1}H-^{17}O correlation spectrum using the $^{1}H\{^{17}O\}$ *D*-RINEPT sequence (see Figure 8b). The most intense cross-peak is detected between carboxylate ^{17}O nuclei and aromatic protons of the terephthalate ligand. The observation of this cross-peak is consistent with the close proximity between these nuclei since according to the crystal structure, the shortest distance between aromatic protons and carboxylate oxygen atoms is 2.46 Å.[7] Furthermore, the presence of this cross peak proves that the dipolar coupling between these ^{1}H and ^{17}O nuclei is not averaged out by the rotational dynamics of the phenylene rings.[34,35] An additional cross-peak reveals the proximities between protons of DMF and ^{17}O nuclei of the carboxylate group. This proximity is consistent with previous studies suggesting that in UiO-66(Zr), some DMF molecules are strongly bound to the inorganic cluster either by coordinating vacancies on Zr^{4+} ions[36,37] or by hydrogen bonding with some Zr–OH groups.[38,39] Lastly, a more weak cross peak between ^{1}H and ^{17}O nuclei of μ_3-OH sites is also detected (not visible on Fig.

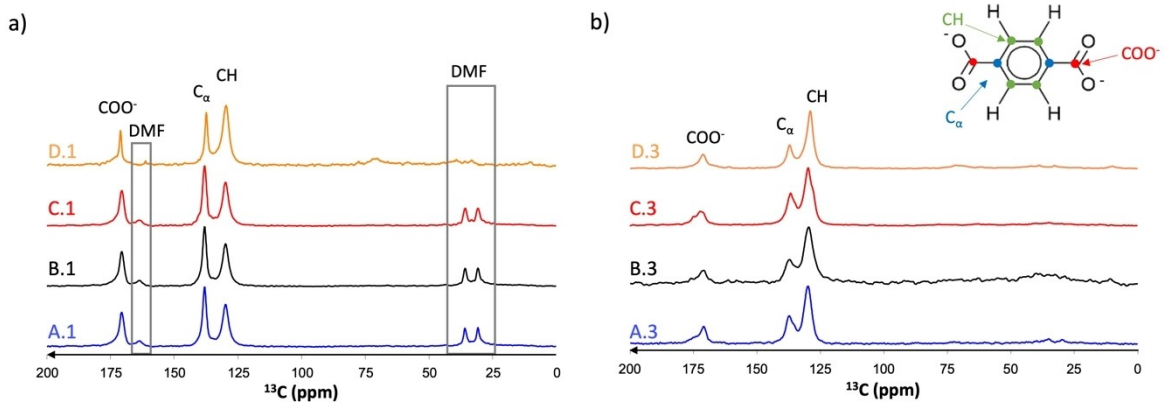

Figure 5. 1D $^{1}H\rightarrow^{13}C$ CPMAS NMR spectra of the samples after the (a) first and (b) third steps recorded at 9.4 T with $\nu_R = 20$ kHz.

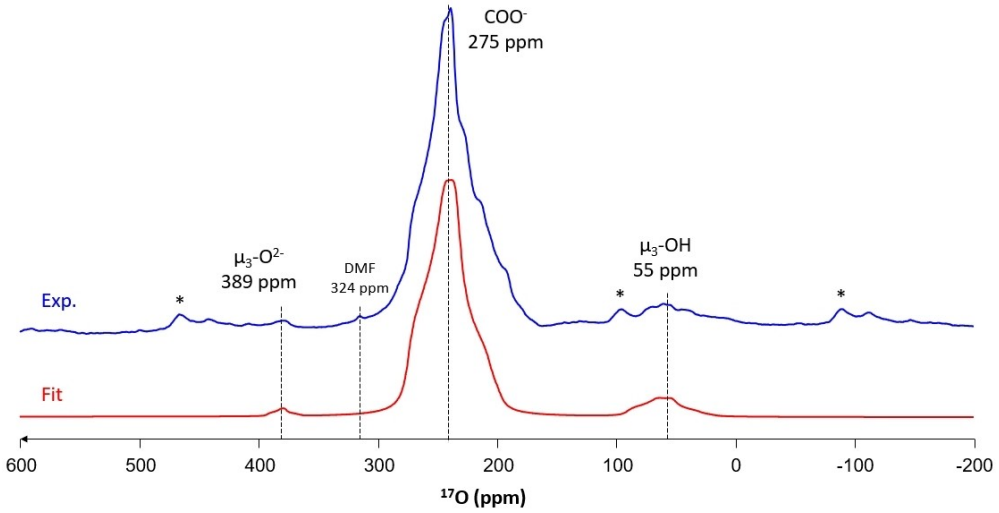

Figure 6. Experimental (blue) and simulated (red) 1D ^{17}O MAS NMR spectrum of UiO-66(Zr) sample A.1 at 18.8 T with $\nu_R = 20$ kHz by averaging 15000 transients. The * symbol denotes spinning side bands.

8a). Its low intensity results from the lower level of ^{17}O enrichment for these sites compared to carboxylate groups. Conversely, no cross peak is detected for μ_3-$^{17}O^{2-}$ nuclei under the analytical conditions used here.

The 1D ^{17}O NMR spectra of the UiO-66(Zr) MOF after the adsorption of water are shown in Figure 7a. These spectra exhibit an extra peak at 0 ppm, which can be assigned to water. As expected, this signal is weak in the case of sample A.2, for which natural abundance water was adsorbed and this spectrum is still dominated by the ^{17}O signal of carboxylate group. Hence, the sample A.2 is still predominantly enriched in the carboxylate oxygen sites. Its 2D ^{17}O 3QMAS spectrum, shown in Figure S4a, indicates that, similarly to the sample A.1, it contains mainly a single type of carboxylate sites (see Figure S5). Nevertheless, following this hydrothermal treatment with non-labeled water (sample A.2), the relative intensity of the μ_3-O^{2-} signal increases at the expense of the COO^- signal (see sample A.2 in Table S1, and Figure S8). This suggests that, overall, an isotopic exchange between the COO^- and μ_3-O^{2-} groups has occurred. Furthermore, an additional resonance assigned to DMF at 324 ppm is detected (see the vertical expansion of the spectra displayed in Figure S6).[40,41] These observations suggest that the ^{17}O nuclei of carboxylate groups of terephthalate ligands can overall be transferred not only to μ_3-O^{2-} sites, but also to water and DMF. ^{17}O-enriched DMF has already been observed in α-$Mg_3(HCOO)_6$ MOF, which had been synthesized in the presence of $H_2{}^{17}O$.[42] Nevertheless, the possibility to transfer ^{17}O nuclei from carboxylate groups to DMF in MOFs had not been reported so far. This overall exchange of O atoms between carboxylate groups and DMF may be favored by the strong bonding of DMF molecules to the inorganic clusters (see above). Conversely, the relative intensity of μ_3-OH signal is not increased (see Table S1). This may stem from a faster exchange of oxygen atoms between μ_3-OH groups

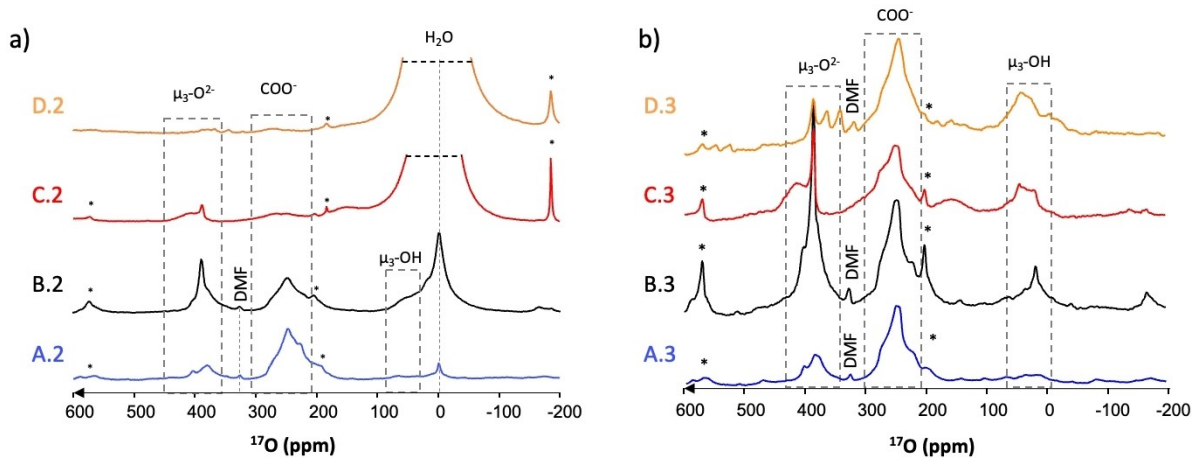

Figure 7. Experimental 1D ^{17}O MAS NMR spectra of the samples of UiO-66(Zr) after the (a) second and (b) third steps recorded at 18.8 T with $\nu_R = 20$ kHz by averaging 7500 transients. The * symbol denotes the spinning side bands. A zoomed-in version of Figure 7a can be found in Figure S6. Note that the spectra in Figure 7b (and spectra A.2 and B.2 from Figure 7a) are normalized according to the number of scans.

and water compared to μ_3-O^{2-} sites. Further analysis at different temperatures and investigations using molecular dynamics simulations would be needed to explore in more detail the dynamical aspects and mechanisms of the oxygen isotopic exchanges occurring within the pores of the MOF, which is beyond the scope of the present work.

In the case of sample B.2, for which ^{17}O-enriched water was adsorbed, the μ_3-O^{2-} signal exhibits higher relative intensity since these sites get enriched in ^{17}O nuclei by the exchange with carboxylate groups and water. Moreover, it should be noted that for sample B.2, there is a difference in intensity and broadening of the water signal compared to samples C.2 and D.2 (despite them having been exposed to the same type of labeled water during the heating step). It seems likely that sample B.2 suffered from different drying conditions compared to the other two samples, during insertion into the glove box prior to NMR experiment. As a result, only the adsorbed water molecules remained, and the more mobile water was evacuated.

The 1D ^{17}O spectra of samples C.2 and D.2 exhibit μ_3-O^{2-} and COO^- signals in agreement with a previous study.[21] These signals indicate that the water ^{17}O nuclei can be transferred to the μ_3-O^{2-} and COO^- groups. Nevertheless, the μ_3-O^{2-} and COO^- signals for these samples are less intense than those of samples A.2 and B.2. These observations are consistent with the fact that these samples were prepared from isotopically unmodified terephthalic acid. The DMF signal is also detected for sample D.2. The ^{17}O NMR spectrum of C.2 exhibits an additional broad resonance centered at ~161 ppm assigned to free terephthalic acid. This resonance is more shielded than that of the terephthalate ligands, for which coordination bonds decrease the electronic density around the ^{17}O nuclei. Furthermore, the local magnetic fields created by currents in the aromatic rings of the terephthalate linkers may also contribute to the shielding of the free terephthalic acid resonance.[43]

After the dehydration step, the water signal decreases for all samples, as seen in Figures 7b and S8. For samples A.3 and B.3, the absolute intensity of the COO^- signal decreases. This decrease can stem from the exchange of ^{17}O nuclei between COO^- sites and water, which is evacuated during the heating at 150 °C. As seen in Figures S4b and S5, the carboxylate ^{17}O signals of samples A.3 and B.3 can still be simulated as a single site with parameters similar to those of samples A.1–2 and B.1–2 (see Table S1). The ^{17}O signal of DMF at 324 ppm is still detected for samples A.3, B.3 and D.3 after the drying step. Furthermore, a cross peak between carboxylate ^{17}O nuclei and DMF protons is visible in the 2D ^{1}H-^{17}O correlation spectrum of sample A.3 shown in Figure 8c. These observations confirms that some ^{17}O-enriched DMF molecules are strongly bound to the inorganic cluster.[16] In addition, the 2D ^{1}H-^{17}O correlation spectrum of sample A.3 exhibits the same cross peaks as those detected for sample A.1 (see Figure 8b).

For samples C.3 and D.3, the elimination of water allows the observation of the μ_3-OH signal. Furthermore, the absolute intensity of the COO^- site is increased (see Fig. S8). This observation suggests that thermal treatment at 150 °C favors the exchange of oxygen atoms between ^{17}O-enriched water and those sites. The broad signal at 161 ppm assigned to free terephthalic acid is also observed in the spectrum of sample C.3.

Furthermore, we acquired 2D ^{17}O 3QMAS spectra of samples C.3 and D.3 with large spectral widths (see Figure 9b and c). These high-resolution 2D spectra allow the observation of ^{17}O NMR signals of μ_3-O^{2-}, COO^-, and μ_3-OH sites, even if the signal-to-noise ratios of the μ_3-O^{2-} and μ_3-OH peaks are low. Furthermore, the 2D ^{1}H{^{17}O} *D*-RINEPT spectrum of sample C.3 shown in Figure 9a exhibits, besides the cross-peak between carboxylate ^{17}O nuclei and aromatic protons, a correlation between the ^{17}O signal centered at 161 ppm and the aromatic protons of the free ligand at 6.3 ppm. This cross-peak confirms that the ^{17}O signal at 161 ppm is assigned to carboxylic groups of free terephthalic molecules. The *D*-RINEPT spectrum also displays cross-peaks between the ^{17}O resonance of μ_3-OH sites at 62 ppm and ^{1}H signals at 7.9 and 2.2 ppm assigned to aromatic protons of free ligand and Zr–OH protons, respectively. The higher intensity of cross-peak between aromatic protons and μ_3-^{17}OH sites for sample C.3 compared to sample A.3 suggests that the free ligands interact with the Zr–OH groups.

Conclusions

We demonstrated in this article using high-field ^{17}O solid-state NMR experiments the possibility to enrich selectively in ^{17}O isotope the carboxylate groups of the UiO-66(Zr) MOF by

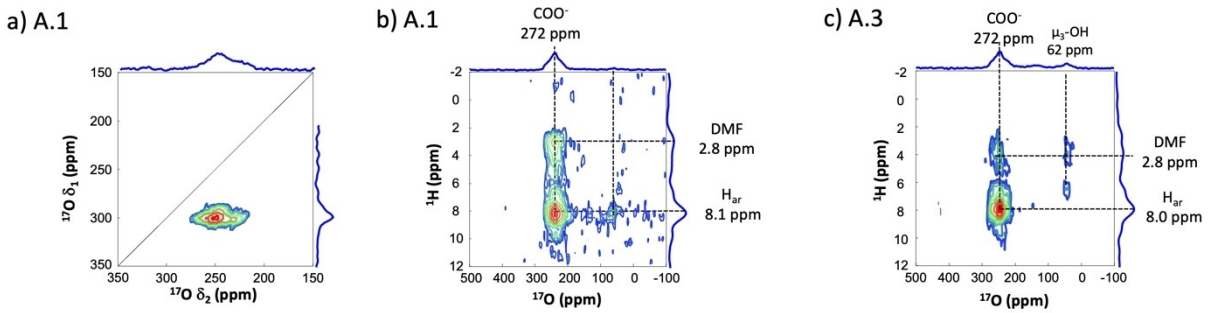

Figure 8. (a) 2D ^{17}O 3QMAS NMR spectrum of sample A.1 and (b, c) 2D ^{1}H{^{17}O} *D*-RINEPT NMR spectra of samples (b) A.1 and (c) A.3 recorded at $B_0 = 18.8$ T and $\nu_R = 20$ kHz, along with their projections.

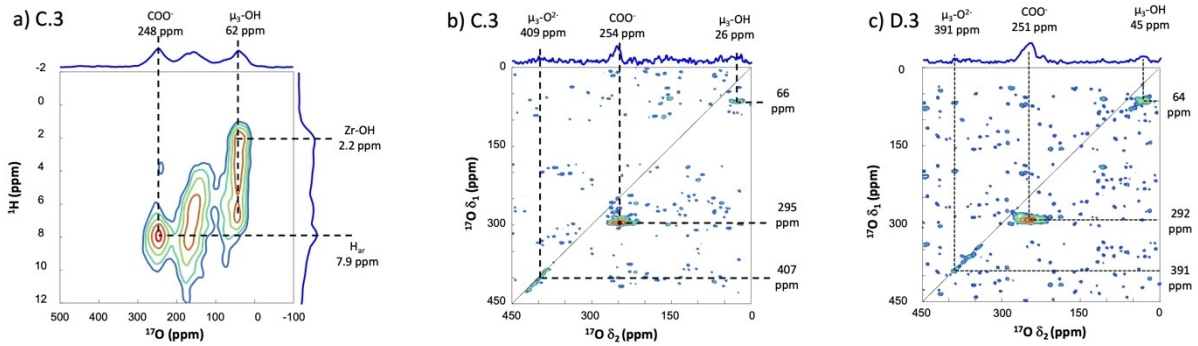

Figure 9. 2D (a) $^{1}H\{^{17}O\}$ *D*-RINEPT and (b, c) ^{17}O 3Q-MAS spectra of samples (a,b) C.3 and (c) D.3 recorded at $B_0 = 18.8$ T and $\nu_R = 20$ kHz. The noted chemical shifts correspond to the maximum peak position (which do not necessarily corresponds to isotropic chemical shifts).

synthesizing this material with terephthalic acid labeled in ^{17}O isotope using mechanochemistry. Furthermore, ^{17}O NMR experiments reveal during hydrothermal treatment an overall transfer of oxygen atoms between carboxylate groups, water and DMF molecules as well as μ_3-O^{2-} and μ_3-OH sites of the inorganic cluster as well as, although the long-range structure of this MOF under this condition is preserved under these conditions. These experimental results demonstrate the lability of Zr–O bonds in UiO-66(Zr) above 50 °C in the presence of water. Therefore, UiO-66(Zr) reacts with water at these temperatures, even if its crystal structure is retained.

Acknowledgements

The Chevreul Institute (FR 2638), Ministère de l'Enseignement Supérieur et de la Recherche, Région Hauts-de-France, FEDER, and IR-RMN are acknowledged for supporting and funding partially this work. Authors are also grateful for funding supported by contract I-site EXPAND MOFFiN. Julien Trébosc is warmly acknowledged his help in the processing. Part of this project has received funding from the European Research Council (ERC) under the European Union's Horizon 2020 research and innovation programme (grant agreement No 772204; 2017 ERC-COG, MISOTOP project).

Conflict of Interests

The authors declare no conflict of interest.

Data Availability Statement

The data that support the findings of this study are available in the supplementary material of this article.

Keywords: UiO-66 · ^{17}O · mechanochemistry · solid-state NMR · water · Zr–O bond

[1] L. Q. Ma, J. M. Falkowski, C. Abney, W. B. Lin, *Nat. Chem.* **2010**, *2(10)*, 838–846. DOI: 10.1038/nchem.738.
[2] H. G. T. Nguyen, N. M. Schweitzer, C. Y. Chang, T. L. Drake, M. C. So, P. C. Stair, O. K. Farha, J. T. Hupp, S. T. Nguyen, *ACS Catal.* **2014**, *4(8)*, 2496–2500. DOI: 10.1021/cs5001448.
[3] M. Q. Zha, J. Liu, Y. L. Wong, Z. T. Xu, *J. Mater. Chem. A* **2015**, *3(7)*, 3928–3934. DOI: 10.1039/c4ta06678b.
[4] M. X. Wu, Y. W. Yang, *Adv. Mater.* **2017**, *29(23)*. DOI: 10.1002/adma.201606134.
[5] P. Horcajada, T. Chalati, C. Serre, B. Gillet, C. Sebrie, T. Baati, J. F. Eubank, D. Heurtaux, P. Clayette, C. Kreuz, J. S. Chang, Y. K. Hwang, V. Marsaud, P. N. Bories, L. Cynober, S. Gil, G. Férey, P. Couvreur, R. Gref, *Nat. Mater.* **2010**, *9(2)*, 172–178. DOI: 10.1038/nmat2608.
[6] Z. R. Herm, B. M. Wiers, J. A. Mason, J. M. van Baten, M. R. Hudson, P. Zajdel, C. M. Brown, N. Masciocchi, R. Krishna, J. R. Long, *Science* **2013**, *340(6135)*, 960–964. DOI: 10.1126/science.1234071.
[7] J. H. Cavka, S. Jakobsen, U. Olsbye, N. Guillou, C. Lamberti, S. Bordiga, K. P. Lillerud, *J. Am. Chem. Soc.* **2008**, *130(42)*, 13850–13851. DOI: 10.1021/ja8057953.
[8] D. Zou, D. Liu, *Mater. Today Chem.* **2019**, *12*, 139–165. DOI: 10.1016/j.mtchem.2018.12.004.
[9] I. Abánades Lázaro, R. S. Forgan, *Coord. Chem. Rev.* **2019**, *380*, 230–259. DOI: 10.1016/j.ccr.2018.09.009.
[10] A. Dhakshinamoorthy, A. Santiago-Portillo, A. M. Asiri, H. Garcia, *ChemCatChem* **2019**, *11(3)*, 899–923, DOI: 10.1002/cctc.201801452.
[11] J. Winarta, B. Shan, S. M. McIntyre, L. Ye, C. Wang, J. Liu, B. Mu, *Cryst. Growth Des.* **2020**, *20(2)*, 1347–1362, DOI: 10.1021/acs.cgd.9b00955.
[12] F, Ahmadijokani, H. Molavi, M. Rezakazemi, S. Tajahmadi, A. Bahi, F. Ko, T. M. Aminabhavi, J. R. Li, M. Arjmand, *Prog. Mater. Sci.* **2022**, *125*, DOI: 10.1016/j.pmatsci.2021.100904.
[13] J. B. DeCoste, G. W. Peterson, H. Jasuja, T. G. Glover, Y. G. Huang, K. S. Walton, *J. Mater. Chem. A* **2013**, *1(18)*, 5642–5650. DOI: 10.1039/c3ta10662d.
[14] I. Bezverkhyy, G. Ortiz, G. Chaplais, C. Marchal, G. Weber, *Microporous Mesoporous Mater.* **2014**, *183*, 156–161.
[15] R. Giovine, F. Pourpoint, S. Duval, O. Lafon, J. P. Amoureux, T. Loiseau, C. Volkringer, *Cryst. Growth Des.* **2018**, *18(11)*, 6681–6693. DOI: 10.1021/acs.cgd.8b00931.
[16] F. Venel, C. Volkringer, O. Lafon, F. Pourpoint, *Solid State Nucl. Magn. Reson.* **2022**, *120*, 101797 DOI: 10.1016/j.ssnmr.2022.101797.
[17] G. P. M. Bignami, Z. H. Davis, D. M. Dawson, S. A. Morris, S. E. Russell, D. McKay, R. E. Parke, D. Iuga, R. E. Morris, S. E. Ashbrook, *Chem. Sci.* **2018**, *9(4)*, 850–859. DOI: 10.1039/c7sc04649a.
[18] D. Carnevale, G. Mouchaham, S. J. Wang, M. Baudin, C. Serre, G. Bodenhausen, D. Abergel, *Phys. Chem. Chem. Phys.* **2021**, *23 (3)*, 2245–2251. DOI: 10.1039/d0cp06064j.
[19] S. E. Ashbrook, Z. H. Davis, R. E. Morris, C. M. Rice, *Chem. Sci.* **2021**, *12(14)*, 5016–5036. DOI: 10.1039/d1sc00552a.
[20] M. Muller, S. Hermes, K. Kaehler, M. W. E. van den Berg, M. Muhler, R. A. Fischer, *Chem. Mater.* **2008**, *20(14)*, 4576–4587. DOI: 10.1021/cm703339h.
[21] P. He, J. Xu, V. V. Terskikh, A. Sutrisno, H. Y. Nie, Y. N. Huang, *J. Phys. Chem. C* **2013**, *117(33)*, 16953–16960. DOI: 10.1021/jp403512m.

[22] W. Xu, N. Hanikel, K. A. Lomachenko, C. Atzori, A. Lund, H. Lyu, Z. Zhou, C. A. Angell, O. M. Yaghi, *Angew. Chem. Int. Ed.* **2023**, *62(16)*. DOI: 10.1002/anie.202300003.
[23] T. X. Métro, C. Gervais, A. Martinez, C. Bonhomme, D. Laurencin, *Angew. Chem. Int. Ed.* **2017**, *56(24)*, 6803–6807. DOI: 10.1002/anie.201702251.
[24] C. H. Chen, I. Goldberga, P. Gaveau, S. Mittelette, J. Spackova, C. Mullen, I. Petit, T. X. Métro, B. Alonso, C. Gervais, D. Laurencin, *Magn. Reson. Chem.* **2021**, *59(9–10)*, 975–990. DOI: 10.1002/mrc.5141.
[25] C. Leroy, T. X. Métro, I. Hung, Z. Gan, C. Gervais, D. Laurencin, *Chem. Mater.* **2022**, *34(5)*, 2292–2312. DOI: 10.1021/acs.chemmater.1c04132.
[26] A. Schaate, P. Roy, P. A. Godt, J. Lippke, F. Waltz, M. Wiebcke, P. Behrens, *Chem. Eur. J.* **2011**, *17(24)*, 6643–6651. DOI: 10.1002/chem.201003211.
[27] T. J. Bastow, S. N. Stuart, *Chem. Phys.* **1990**, *143(3)*, 459–467. DOI: 10.1016/0301-0104(90)87025-7.
[28] J. P. Amoureux, C. Fernandez, S. Steuernagel, *J. Magn. Reson.* **1996**, *123(1)*, 116–118. DOI: 10.1006/jmra.1996.0221.
[29] R. Giovine, J. Trébosc, F. Pourpoint, O. Lafon, J. P. Amoureux, *J. Magn. Reson.* **2019**, *299*, 109–123. DOI: 10.1016/j.jmr.2018.12.016.
[30] A. Venkatesh, M. P. Hanrahan, A. J. Rossini, *Solid State Nucl. Magn. Reson.* **2017**, *84*, 171–181. DOI: 10.1016/j.ssnmr.2017.03.005.
[31] A. Brinkmann, A. P. M. Kentgens, *J. Am. Chem. Soc.* **2006**, *128(46)*, 14758–14759. DOI: 10.1021/ja065415k.
[32] B. M. Fung, A. K. Khitrin, K. Ermolaev, *J. Magn. Reson.* **2000**, *142(1)*, 97–101. DOI: 10.1006/jmre.1999.1896.
[33] D. Massiot, F. Fayon, M. Capron, I. King, S. Le Calve, B. Alonso, J. O. Durand, B. Bujoli, Z. H. Gan, G. Hoatson, *Magn. Reson. Chem.* **2002**, *40(1)*, 70–76. DOI: 10.1002/mrc.984.
[34] A. E. Khudozhitkov, D. I. Kolokolov, A. G. Stepanov, *J. Phys. Chem. C* **2018**, *122(24)*, 12956–12962. DOI: 10.1021/acs.jpcc.8b03701.
[35] A. Gonzalez-Nelson, F. X. Coudert, M. A. van der Veen, *Nanomaterials* **2019**, *9(3)*, Review. DOI: 10.3390/nano9030330.
[36] M. Taddei, J. A. van Bokhoven, M. Ranocchiari, *Inorg. Chem.* **2020**, *59(11)*, 7860–7868. DOI: 10.1021/acs.inorgchem.0c00991.
[37] S. Oien, D. Wragg, H. Reinsch, S. Svelle, S. Bordiga, C. Lamberti, K. P. Lillerud, *Cryst. Growth Des.* **2014**, *14(11)*, 5370–5372. DOI: 10.1021/cg501386j.
[38] Y. An, A. Kleinhammes, P. Doyle, E. Y. Chen, Y. Song, A. J. Morris, B. Gibbons, M. Cai, J. K. Johnson, P. B. Shukla, M. N. Vo, X. Wei, C. E. Wilmer, J. P. Ruffley, L. L. Huang, T. M. Tovar, J. J. Mahle, C. J. Karwacki, Y. L. Wu, *Phys. Chem. Lett.* **2021**, *12(2)*, 892–899. DOI: 10.1021/acs.jpclett.0c03504.
[39] S. Wang, J. S. Lee, M. Wahiduzzaman, J. Park, M. Muschi, C. Martineau-Corcos, A. Tissot, K. H. Cho, J. Marrot, W. Shepard, G. Maurin, J. S. Chang, C. Serre, *Nat. Energy* **2018**, *3(11)*, 985–993. DOI: 10.1038/s41560-018-0261-6.
[40] M. I. Burgar, T. E. Stamour, D. Fiat, *J. Phys. Chem.* **1981**, *85(5)*, 502–510. DOI: 10.1021/j150605a011.
[41] I. P. Gerothanassis, C. Vakka, *J. Org. Chem.* **1994**, *59(9)*, 2341–2348. DOI: 10.1021/jo00088a013.
[42] V. Martins, J. Xu, X. Wang, K. Chen, I. Hung, Z. Gan, C. Gervais, C. Bonhomme, S. Jiang, A. Zheng, B. E. G. Lucier, Y. N. Huang, *J. Am. Chem. Soc.* **2020**, *142(35)*, 14877–14889. DOI: 10.1021/jacs.0c02810.
[43] A. Nandy, A. C. Forse, V. J. Witherspoon, J. A. Reimer, *J. Phys. Chem. C* **2018**, *122(15)*, 8295–8305. DOI: 10.1021/acs.jpcc.7b12628.

Manuscript received: August 21, 2023
Version of record online: January 16, 2024